

Constraints on Heavy Asymmetric and Symmetric Dark Matter from the Glashow Resonance

Qinrui Liu,^{1,2,3,*} Ningqiang Song,^{4,†} and Aaron C. Vincent^{1,2,3,‡}

¹*Department of Physics, Engineering Physics and Astronomy,
Queen's University, Kingston ON K7L 3N6, Canada*

²*Arthur B. McDonald Canadian Astroparticle Physics Research Institute, Kingston ON K7L 3N6, Canada*

³*Perimeter Institute for Theoretical Physics, Waterloo ON N2L 2Y5, Canada*

⁴*Institute of Theoretical Physics, Chinese Academy of Sciences, Beijing, 100190, China*

(Dated: June 24, 2024)

The decay of asymmetric dark matter (ADM) can lead to distinct neutrino signatures characterized by an asymmetry between neutrinos and antineutrinos. In the high-energy regime, the Glashow resonant interaction $\bar{\nu}_e + e^- \rightarrow W^-$ yields an increase in sensitivity to the neutrino flux, and stands out as the only way of discerning the antineutrino component in the diffuse high-energy astrophysical neutrino flux. This offers a unique opportunity in the search for dark matter with masses above the PeV scale. We examine the neutrino signal stemming from ADM decay and set the first stringent constraints on ADM lifetime τ_X . For ADM with mass $m_X \gtrsim 10$ PeV, we find $\tau_X \lesssim 10^{29}$ s using the data from the recent IceCube search for Glashow resonance events. Our projections further show that sensitivities at the forthcoming IceCube-Gen2 could approach 10^{30} s, depending on the decay channel. The current constraints on symmetric dark matter decay to neutrinos are also improved by up to a factor of 3 thanks to the Glashow resonance.

Introduction — High-energy astrophysical neutrinos in the TeV-PeV range have been detected in large Cherenkov telescopes, most notably IceCube [1]. Detection is primarily through deep inelastic scattering (DIS) with nucleons via charged current (CC) or neutral current (NC) interactions, producing event morphologies that are recognized as showers (or cascades), tracks, or double cascades in or near the detector. Although the morphologies allow some reconstruction of the flavor of high energy neutrinos, the identification of the neutrino CP eigenstates in these interactions remains impossible. The only way to pin down the antineutrino component from the total neutrino flux at high energies is the so-called Glashow resonance (GR) [2], *i.e.* the resonant scattering of $\bar{\nu}_e$ on electrons in the detector $\bar{\nu}_e + e^- \rightarrow W^-$, which dramatically enhances the cross section for neutrino energies near 6.3 PeV.

Such an event was first reported by IceCube as a partially contained cascade with a reconstructed energy of 6.05 ± 0.72 PeV [3]. The detection of GR events with neutrino telescopes such as IceCube can grant a deeper understanding of astrophysical processes [4–18], and opens the door to new physics searches, e.g. neutrino decay and Lorentz invariance violation [19–22]. In a variety of models, dark matter (DM) interacts primarily with neutrinos, enabling the decay or annihilation of DM into neutrinos [23–32]. In such scenarios, the direct detection of DM becomes challenging, although indirect searches for neutrino-DM elastic scattering benefit from an enhanced cross section at high energies [33]. Searches for neutrino signals from DM annihilation [34] or decay [35] have also

led to strong constraints on these models. Decay to neutrinos is particularly well-constrained at very high energies thanks to the growing neutrino-nucleus cross section and the presence of gamma rays from electroweak corrections.

As the GR breaks the degeneracy between neutrinos and antineutrinos, it is a sensitive probe of asymmetric dark matter (ADM), an alternative to the widely-studied weakly interacting massive particles (WIMPs). Asymmetric models were proposed to connect the relic abundance of DM to the baryon asymmetry in the Universe [36], but are not generically tied to baryogenesis. If the dark sector's asymmetry is linked to the standard model (SM) sector, then decay could give rise to an asymmetry between SM decay products [37–43], including neutrinos [44, 45]. Fig. 1 shows predictions from a few such scenarios overlaid on observational data. These scenarios will be described later in this text.

In this work, we will exploit the enhanced cross section in the Glashow region to 1) improve on existing constraints on the decay of *symmetric* dark matter to $\bar{\nu}\nu$, and 2) derive new constraints on *asymmetric* dark matter decay to a number of neutrinophilic channels, setting stringent constraints on the ADM lifetime at $\tau_X \lesssim 10^{29}$ s for ADM mass $m_X \gtrsim 10$ PeV. Neutrinos produced from electroweak radiation preserve information about the asymmetry, and allow us to cover a mass range between 10^7 and 10^{10} GeV. We will present constraints from currently available IceCube data, and projected sensitivities from the upcoming IceCube-Gen2.

We begin by presenting ADM models examined here, then describe our analysis framework, before placing constraints on these models. We conclude with sensitivity projections from upcoming neutrino observatories, and a short discussion.

Heavy Asymmetric Dark Matter Decay — Al-

* qinrui.liu@queensu.ca

† songnq@itp.ac.cn

‡ aaron.vincent@queensu.ca

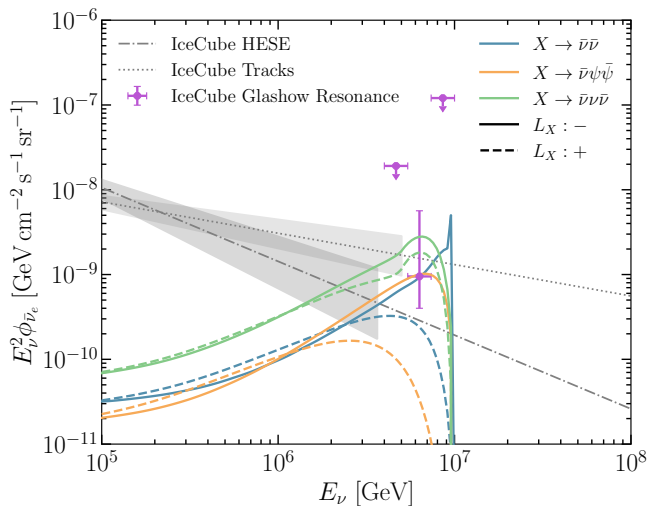


FIG. 1. Expected spectra of with the three decay modes, *i.e.* $X \rightarrow \bar{\nu}(\nu)\nu\nu$ (blue), $X \rightarrow \bar{\nu}(\nu) + \psi\bar{\psi}$ (orange) and $X \rightarrow \bar{\nu}(\nu) + \nu\bar{\nu}$ (green) for $m_X = 20$ PeV when the lifetime $\tau_X = 10^{29}$ s. A solid line corresponds to the mode with a negative lepton number and the dashed line corresponds to a positive lepton number. The IceCube GR observation [3] is shown as purple points. Gray lines are IceCube diffuse astrophysical neutrino measurements of high-energy starting events (dash-dotted) [46] and through-going muon tracks (dotted) [47], which are to the softest and hardest spectra with current IceCube measurements. For IceCube diffuse astrophysical neutrino measurements shown here, we assume $\bar{\nu}_e$ constitutes 1/6 of the total flux.

though some of the first ADM models predicted new particles in the 5–15 GeV mass range [36], models exist spanning a vast range of scales, and heavy ADM in particular has been widely explored [37–39, 43, 48–51]. Such constructions can be naturally realized in various scenarios, *e.g.* if the SM and the dark sector were never in thermal equilibrium and they both originate from the decay of a heavy mother particle with nonzero primordial baryon/lepton number asymmetry [48–50], or the thermally produced ADM goes through self-annihilating process producing lighter dark particles and depleting its abundance to the level observed today [43]. Asymmetric heavy dark quarks can also be left over when the temperature of the first order phase transition is well below the mass of dark quarks, allowing the symmetric component to further annihilate during the contraction of false vacuum pockets [51]. The mass of AMD is effectively unconstrained in these scenarios, so we treat m_X as a free parameter.

ADM typically carries $B - L$ (baryon minus lepton) numbers, and can transfer an asymmetry between the dark sector and SM via operators of the form

$$\mathcal{O}_{\text{ADM}} = \frac{\mathcal{O}_X \mathcal{O}_{\text{SM}}}{\Lambda^{m+n-4}}, \quad (1)$$

where the dark sector \mathcal{O}_X and SM \mathcal{O}_{SM} operators have dimensions m and n respectively [43, 44]. In general, in

order to allow for asymmetric decay to neutrinos while the lepton number conservation is respected, DM X has to be charged under SM $SU(2)$. We intend to be model-independent and focus on a set of representative benchmark operators that lead to neutrino decay, as listed in Table. I. We focus on dominant lowest-dimension operators that produce distinct GR signals depending on the $B - L$ charge of the DM. For all those scenarios, DM X carries a lepton number L_X . In Table. I, L is the SM lepton doublet and Φ is a heavy scalar doublet which can be integrated out [44]. A scalar DM X can decay through the 2-body process to a neutrino and a dark fermion ψ , *i.e.* $X \rightarrow \bar{\nu}(\nu) + \psi$ (B1) or two neutrinos $X \rightarrow \bar{\nu}\bar{\nu}(\nu\nu)$ (B2). The last two operators can arise from the operator $Xl\phi$ and $\frac{1}{\Lambda^{3n-3}}\phi\psi^n$ with the heavy scalar field ϕ integrated out [45, 52]. This leads to a multi-body decay process for the fermionic DM $X \rightarrow \bar{\nu}(\nu) + 2n\psi$. At the lowest order $n = 1$, the decay produces a neutrino or antineutrino, depending on the lepton number carried by X (B3). The fermion ψ could be a new particle, or from the SM; if $\psi = \nu$ then X decays to three neutrinos (B4).

High-Energy $\bar{\nu}_e$ Flux from ADM — Assuming ADM makes up all DM, we compute the expected high-energy $\bar{\nu}_e$ flux from ADM in the Galactic Halo and beyond the Milky Way via decay channels discussed above.

For the Galactic contribution, the expected neutrino flux depends on the direction. The averaged contribution from the Galactic Halo with a solid angle coverage Ω for DM with mass m_X and lifetime τ_X can be written as

$$\frac{d\Phi_{\bar{\nu}_e}^{\text{gal.}}}{dE_\nu} = \frac{1}{4\pi m_X \tau_X} \sum_\alpha^3 \frac{dN_{\bar{\nu}_\alpha}^{\text{ch}}}{dE_\nu} \frac{\mathcal{D}(\Omega)}{\Omega} P_{\bar{\nu}_\alpha \rightarrow \bar{\nu}_e}, \quad (2)$$

where the D-factor $\mathcal{D} = \int d\Omega \int_{\text{los}} \rho_X [r(s, l, b)] ds$ represents the column density of DM along the line of sight (los) covered in Ω . ρ_X is the galactic DM distribution as a function of the galactocentric distance $r = \sqrt{s^2 + R_\odot^2 - 2sR_\odot \cos l \cos b}$, where l and b correspond to the Galactic latitude and longitude. We adopt the generalized Navarro-Frenk-White (gNFW) profile with a slope parameter 1.2, local DM density 0.4 GeV/cm^3 and a scale radius 20 kpc [53]. The full-sky coverage $\Omega = 4\pi$ yields $\mathcal{D} = 2.63 \times 10^{23} \text{ GeV cm}^{-2} \text{ sr}$. Switching from the gNFW profile to a cored profile only introduces a $\lesssim 20\%$ difference. $dN_{\bar{\nu}_\alpha}^{\text{ch}}/dE_\nu$ is the energy spectrum of neutrinos produced in the decay of a single DM particle via a specific decay channel to $\bar{\nu}_\alpha$, where $\alpha \in \{e, \mu, \tau\}$. For each decay channel, we assume a flavor-universal production of neutrinos. Since we include the products of the electroweak showers when computing the energy spectrum, universal primary production does not result in the same spectrum for each flavor.

As propagation is incoherent and over long distances, the average flavour oscillation probability from $\bar{\nu}_\alpha$ to $\bar{\nu}_e$ is $P_{\bar{\nu}_\alpha \rightarrow \bar{\nu}_e} = \sum_i |U_{ei}|^2 |U_{\alpha i}|^2$, where U is the Pontecorvo–Maki–Nakagawa–Sakata (PMNS) matrix. An averaged neutrino oscillation effect leads to a $\sim 1/3$ contribution from each flavor to the total flux. In prac-

Benchmark	B1 (scalar X)	B2 (scalar X)	B3 (fermion X)	B4 (fermion X)
$\mathcal{O}_{X \rightarrow \nu}$	$\frac{1}{\Lambda} X \psi L \Phi$	$\frac{1}{\Lambda^2} X (L \Phi)^2$	$\frac{1}{\Lambda^2} X L \psi^2$	$\frac{1}{\Lambda^2} X L L \nu^c$
Decay	$X \rightarrow \bar{\nu} \psi / \nu \psi$	$X \rightarrow \bar{\nu} \bar{\nu} / \nu \nu$	$X \rightarrow \bar{\nu} \psi \bar{\psi} / \nu \psi \bar{\psi}$	$X \rightarrow \bar{\nu} \nu \bar{\nu} / \nu \nu \bar{\nu}$

TABLE I. Operators of the lowest dimensions and their corresponding neutrino-dominant decay modes. The nature of X is indicated in each case. L is the Standard Model lepton doublet, and ψ represents a fermion that could be part of the SM, or of an extended dark sector.

tice, we adopt the best-fit oscillation parameters from NuFIT5.3 [54, 55] to compute this probability.

The extragalactic DM contributes to the isotropic neutrino flux is

$$\frac{d\Phi_{\bar{\nu}_e}^{\text{ext. gal.}}}{dE_\nu} = \frac{\Omega_X \rho_c}{4\pi m_X \tau_X} \sum_\alpha^3 \int_0^\infty \frac{dN_{\bar{\nu}_\alpha}^{\text{ch}}}{dE'_\nu} \frac{dz}{H(z)} P_{\bar{\nu}_\alpha \rightarrow \bar{\nu}_e}, \quad (3)$$

where $\Omega_X = 0.229$ is the DM density in the Universe, ρ_c is the Universe critical density and z is the redshift. $E'_\nu \equiv (1+z)E_\nu$ is the redshifted neutrino energy and $H(z) = H_0 \sqrt{(1+z)^3 \Omega_m + \Omega_\Lambda}$ is the Hubble expansion rate, for which we use $H_0 = 67.4 \text{ km s}^{-1} \text{ Mpc}^{-1}$, $\Omega_m = 0.315$ and $\Omega_\Lambda = 0.685$ [56].

We sum the galactic contribution in Eq. (2) and the extra-galactic contribution in Eq. (3) to find the angular-averaged neutrino flux from ADM decay. As the DM mass considered in this work is well above the electroweak scale, final-state radiation will modify the neutrino spectrum, softening the primary neutrino spectrum, and producing an additional lower energy ν and $\bar{\nu}$ component from electroweak showers. With these corrections, the energy spectrum of $\bar{\nu}_\alpha$ is

$$\frac{dN_{\bar{\nu}_\alpha}^{\text{ch}}}{dE_\nu}(E_\nu) = \sum_i \int_{E_\nu/m_X}^1 \frac{1}{ym_X} \frac{df_i}{dy} D_i^{\bar{\nu}_\alpha}(x; ym_X) dy, \quad (4)$$

where the sum on i goes over each (anti)neutrino produced in the uncorrected decay, including a sum over flavors. f_i is the distribution function for decay product i , which we provide in Appendix A. We implement the fragmentation functions $D_i^j(x; ym_X)$ from `HDMSpectrum` [57] where y represents the fraction of energy taken away by particle i in the DM mass and $x \equiv E_j/(ym_X)$ is the energy fraction deposited to the final particle j from the initial particle energy. The subsequent evolution such as hadronization and showering handled by `PYTHIA8.2` [58–60] is also included in the fragmentation functions.

The $\bar{\nu}_e$ spectra from the benchmark decay modes are shown in Fig. 1. The electroweak corrections tend to broaden the Dirac delta spectrum in two-body decay, and generate a $\bar{\nu}_e$ flux even when antineutrinos are absent in the initial decay products. If X carries negative lepton number $L_X < 0$ which tends to decay more to antineutrinos, the flux is more peaked at high energies. On the contrary, if $L_X > 0$ the $\bar{\nu}_e$ spectrum is more

suppressed at the highest energies and peaks at lower energies. At $E_{\bar{\nu}_e}/m_X \lesssim 10^{-2}$, the $\bar{\nu}_e$ spectral for $L_X > 0$ and $L_X < 0$ converge. This means that GR loses the ability to pin down the asymmetry and lepton number of X when $m_X \gtrsim \text{EeV}$.

Current IceCube Data — We set constraints on ADM with publicly available IceCube data [3]. The measured flux is under the assumption of $(\nu : \bar{\nu}) = (1 : 1)$ and a flavor ratio of $(\nu_e : \nu_\mu : \nu_\tau) = (1 : 1 : 1)$ at Earth. The segmented differential flux reported in Ref. [3] covers the energy range [4, 10] PeV assuming an E^{-2} power-law spectrum within each bin. This analysis includes the effect of Doppler broadening which induces a $\sim 20\%$ broadening on the cross section of the GR due to electronic motions [61]. When computing the limits with current observations, we integrate the reported differential flux limits over each bin to obtain $\Phi_{\text{obs},i}$, and compare these with the expected flux per bin $\Phi_{\text{exp},i}$ for each set of model and background parameters. The uncertainty can be similarly integrated to obtain $\sigma_{\Phi_{\text{obs},i}}^2$.

The measured $\bar{\nu}_e$ flux receives contributions mainly from two sources: the diffuse astrophysical neutrino flux and the flux from DM decay. We ignore the atmospheric neutrino flux which is negligible next to the astrophysical flux at PeV energies. The main background is therefore from the isotropic astrophysical neutrino flux which is typically modeled as a power-law $d\Phi_\nu^{\text{astro.}}/dE_\nu = \phi_0 (E_\nu/100 \text{ TeV})^{-\gamma}$, where ϕ_0 is the flux normalization and γ is the spectral index. In this work, we fix the values to the best fits of the 7.5yr high-energy starting events (HESE) analysis [46]. We assume that $\bar{\nu}_e$ makes up 1/6 of the total astrophysical flux at Earth, corresponding to the equal-flavor assumption used in the HESE analysis. This is consistent with a general scenario in which these neutrinos are produced from π^\pm decays at the source and experience oscillation during the propagation. Since the statistics of PeV neutrinos are low, the spectral index plays an important role in the predicted event rate. We will discuss the effects of the spectral index and the $\bar{\nu}_e$ fraction when presenting the results.

The expected integrated flux in each energy bin i from these two sources is therefore

$$\Phi_{\text{exp},i} = \int_{E_{\text{min},i}}^{E_{\text{max},i}} \left[\frac{d\Phi_\nu^{\text{DM}}}{dE_\nu} + \frac{d\Phi_\nu^{\text{astro.}}}{dE_\nu} \right] dE_\nu. \quad (5)$$

To evaluate the limits on the DM lifetime for a given DM

mass m_X , we define a Gaussian likelihood such that

$$-2\ln\mathcal{L}(\tau_X, m_X) = \sum_i^3 \frac{(\Phi_{\text{exp},i} - \Phi_{\text{obs},i})^2}{\sigma_{\Phi_{\text{obs},i}}^2}. \quad (6)$$

We construct the test statistic

$$\text{TS} = 2\ln[\mathcal{L}(\hat{\tau}_X, m_X) / \mathcal{L}(\tau_X, m_X)], \quad (7)$$

where $\hat{\tau}_X$ is the value that maximizes Eq. (6). Assuming Wilks's theorem holds, we obtain the 90% limit on the lifetime for each individual mass by finding the value of τ_X for which $\text{TS} = 2.71$.

Future Projections — We can also study the detectability of ADM decay at the next-generation neutrino telescopes. There is a suite of facilities under construction or proposed for the detection of high-energy astrophysical neutrinos with substantially larger exposure and event statistics. Here we focus on IceCube-Gen2, which will extend the current IceCube detector to a volume of 8 km³ [65]. We will discuss other next-generation experiments in Appendix B.

We focus on the partially-contained event selection [3], which is the selection used for the IceCube GR observation and enlarges the effective area by approximately a factor of 2 in the GR energy window compared to the contained event selection (HESE, [46]), which in turn leads to a twofold increase in the event rate over HESE. The expected number of (partially) contained events depends on the the detector effective volume and exposure time of the experiment. Therefore, the partially-contained event rate at a future neutrino telescope with a instrumental volume V can be scaled from that of IceCube (~ 1 km³ in size) by a factor of $\sim 2 (V/1 \text{ km}^3)$. We use the public Monte Carlo (MC) simulation of HESE [46]¹ to compute the latter, which includes reconstruction effects such as energy reconstruction and misidentification, as well as ice and detector systematics. Since the HESE MC does not account for Doppler broadening and initial photon radiation, we include these with an appropriate reweighting. Details are provided in Appendix C.

We build our projection on the expectation that GR events can be identified on an event-wise basis. As discussed in Ref. [17], the dominant hadronic decay channel $W^- \rightarrow \text{hadrons}$ and the $W^- \rightarrow \mu^- + \bar{\nu}_\mu$ channel should be differentiable from DIS events. The former gives rise to a distinct signal: mesons decay into muons with energies of tens of GeV whose Cherenkov photons are visible as early pulses. This distinguishes them from a charged current DIS cascade [3]. Neutral current DIS events are also expected to create hadronic cascades, but they require the incoming neutrino to be much more energetic to deposit similar amount of energy in the detector. This is suppressed due to the low astrophysical flux expected at

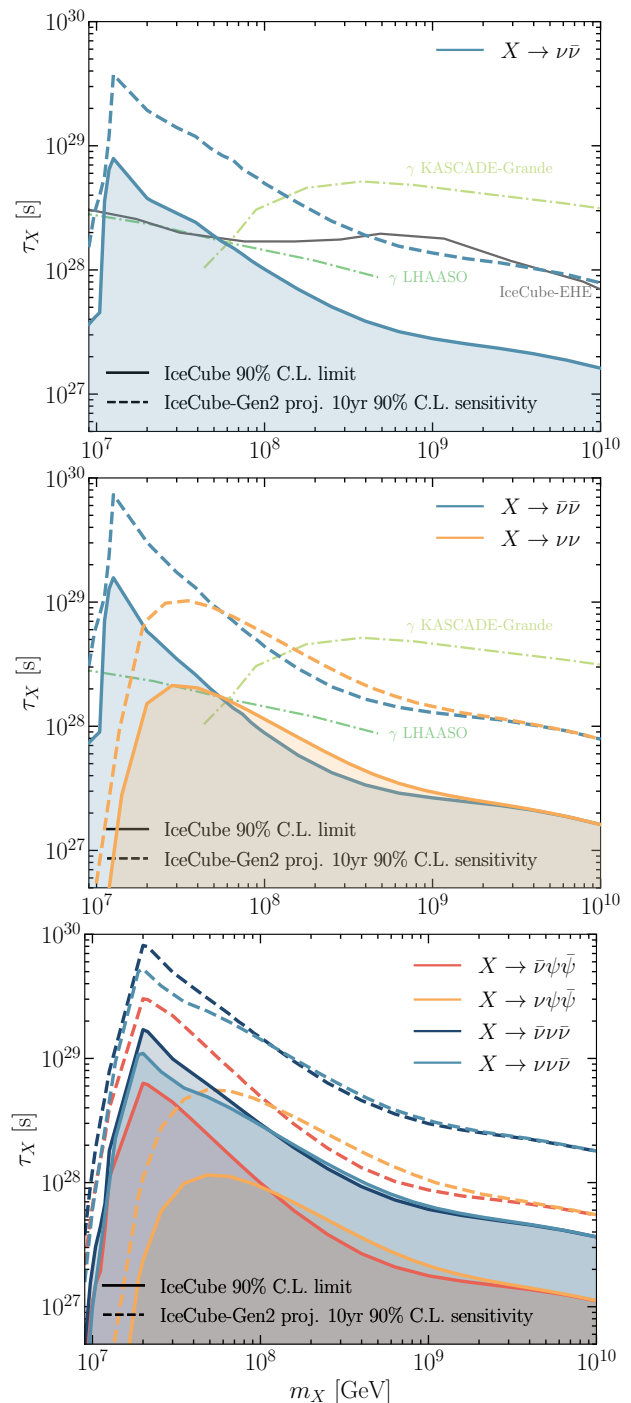


FIG. 2. **Top:** 90% C.L. constraints on the lifetime of X in $X \rightarrow \bar{\nu}\nu$ decay with the current IceCube observation of GR (shaded regions), and the projected sensitivities in the future with 10 yr exposure of IceCube-Gen2 (dashed). We also show the corresponding limits with neutrino and gamma-ray observations from Ref. [35] derived from the diffuse gamma flux limit by KASCADE-Grande [62] (light green) and the extremely-high-energy (EHE) astrophysical neutrino flux limit by IceCube [63] (gray), as well as the LHAASO limit [64] (dark green). **Middle and bottom:** 90% C.L. constraints on the lifetime of ADM for the three decay modes. The gamma-ray limits here may also apply to the scenario of $X \rightarrow \bar{\nu}\nu(\nu\nu)$.

¹ <https://github.com/icecube/HESE-7-year-data-release>

higher energies. The W decay channel to muons results in a track without a cascade at the primary vertex, in contrast to charged current ν_μ DIS interactions in which the nucleon is disintegrated. This contribution is nevertheless subdominant as the branching ratio to muons rate is much lower than to hadrons.

In order to compute the sensitivity, we perform a binned likelihood ratio analysis based on the Poisson likelihood of Glashow-induced cascades (cas) and tracks (tr) in each of the three bins defined in Ref. [3]:

$$\mathcal{L} = \prod_i^3 \mathcal{L}_i^{\text{cas}} \prod_j^3 \mathcal{L}_j^{\text{tr}} = \prod_i^3 \frac{\mu_i^{\text{cas}}}{k_i^{\text{cas}}!} e^{-\mu_i^{\text{cas}}} \prod_j^3 \frac{\mu_j^{\text{tr}}}{k_j^{\text{tr}}!} e^{-\mu_j^{\text{tr}}}. \quad (8)$$

Here, μ represents expected events per bin, and k correspond to the observed GR counts. In each case, $\mu_i = \mu_i^{\text{DM}} + \mu_i^{\text{astro}}$ consists of contributions from the DM and the diffuse astrophysical neutrino flux and can be computed as

$$\mu_i^k = T \int_{\Delta E_i} \int_{E_\nu} A_{\text{eff}}(E_\nu) \frac{d\Phi_\nu^k}{dE_\nu} \frac{d\mathcal{P}}{dE_{\text{reco}}} dE_\nu dE_{\text{reco}}, \quad (9)$$

where $k = \text{DM or astro}$, and T is the exposure time of the experiment. The effective area A_{eff} depends on the interaction type, the neutrino energy and the zenith angle. Since we are considering a direction-averaged flux, A_{eff} here is also averaged in zenith angle. $d\mathcal{P}/dE_{\text{reco}}$ takes into account the reconstruction effect, indicating the probability of observing an event of E_{reco} from a incoming neutrino with energy E_ν . ΔE_i is the width of the reconstructed energy in bin i .

To compute the sensitivity, the test statistic has $\text{TS} = 2\ln[\mathcal{L}(\tau_X, m_X)/\mathcal{L}_{\text{null}}]$ in which $\mathcal{L}_{\text{null}}$ is the likelihood value of the null hypothesis where there is no contribution from the DM, *i.e.* τ_X is infinite.

Results — We first present updated constraints on symmetric DM decay, $X \rightarrow \nu\bar{\nu}$, in the top panel of Fig. 2. Thanks to the Glashow-enhanced cross section, our constraint on the dark matter lifetime surpasses the IceCube extremely-high-energy astrophysical neutrino flux limit [63] in the 10 – 50 PeV mass window, and is up to a factor of 3 stronger.

The constraints on ADM lifetime obtained with the IceCube GR dataset are shown in the bottom two panels of Fig. 2 for the representative decay modes listed in Table I. For B1 (therefore also B2) and B3, when the DM mass is around the GR energy, the constraint for the antineutrino decay $L_X < 0$ is about two orders of magnitude stronger than $L_X > 0$. The difference shrinks as the ADM mass increases and eventually the two branches intersect at $m_X \sim 100$ PeV. For $m_X \gtrsim \text{EeV}$ the difference between $L_X < 0$ and $L_X > 0$ decay diminishes, and constraints on ADM become indistinguishable from those on symmetric particles, consistent with the $\bar{\nu}_e$ spectrum in Fig. 1. On the other hand, the constraints on $L_X < 0$ and $L_X > 0$ decay branches in B4 are always very similar regardless of m_X , as the decay spectra are

less distinguishable. Scenarios with even more symmetric final states should in turn make any CP asymmetry more difficult to identify.

At high energies, electroweak corrections also give rise to photons that can be observed at gamma-ray telescopes; these spectra are of course insensitive to the $\nu : \bar{\nu}$ ratio. In the panels of Fig. 2 that depict 2-body final states, we also show the derived gamma-ray constraints from LHAASO [64] and KASCADE-Grande [35, 62]. These gamma-ray constraints are up to an order of magnitude stronger for masses above 100 PeV. However, this channel remains insensitive to the sign of the $B - L$ number and hence to any asymmetry in the dark sector.

The projected sensitivities with 10 yr IceCube-Gen2 exposure are also shown in Fig. 2 as dashed lines. They have similar mass dependence as the current constraints, achieving a factor of 5 improvement in sensitivity. We find that the lifetime sensitivity scales with the exposure by the relation $\tau_X \propto \mathcal{E}^{0.59}$ where \mathcal{E} is the exposure. The combination of future neutrino telescopes will of course further improve the sensitivity.

The constraints on decaying dark matter have mild dependence on the neutrino spectral index γ and the $\bar{\nu}_e$ fraction $f_{\bar{\nu}_e}$ of the diffuse astrophysical flux. As displayed in Fig. 1, current measurements of the diffuse astrophysical flux report spectral indices vary from 2.37 (throughgoing muons) to 2.87 (HESE) [46, 47]. Fig. 2 assumes $\gamma = 2.87$. Using $\gamma = 2.37$ gives a fivefold increase in the astrophysical flux in the GR energy range, leaving less room for a DM signal and an improvement of ~ 2 in the limits. Future projections work in the opposite direction, as Asimov data would give a larger background, and thus a *lower* sensitivity if the astrophysical spectrum is harder.

In typical astrophysical production scenarios, the fraction of electron antineutrinos $f_{\bar{\nu}_e}$ can range from 0 to $\lesssim 20\%$ [14]. We find that varying $f_{\bar{\nu}_e}$ from 1/6 to 0 leads to a factor ~ 1.2 decrease in the lifetime constraints and a factor ~ 5 improvement in the lifetime sensitivity.

Conclusions — In this work, we have exploited the large increase in neutrino-electron cross section at the Glashow resonance to place leading limits on dark matter decays to neutrino pairs, and have placed the first constraints on heavy ADM decaying to neutrinos. As GR provides unique opportunities for disentangling neutrinos and antineutrinos, current IceCube data sets the ADM lifetime to be longer than $10^{27} - 10^{29}$ s for $m_X \gtrsim 10$ PeV depending on the decay modes. Thanks to the GR, constraints place here are competitive with—and in some ranges, stronger than—those from gamma ray searches for decay to electromagnetically charged final states such as $b\bar{b}$, $\tau^+\tau^-$, or e^+e^- [64]. Even stronger sensitivities will be achieved in the near future with the upcoming generation of neutrino telescopes which provide considerably larger exposure than IceCube.

Distinct from charged cosmic rays, neutrinos directly point back to their sources, and unlike gamma rays, they

travel without being attenuated and carry information about the initial CP state. A strong case for complementarity exists: because dark matter in this mass range would produce a flux of gamma rays and neutrinos, a simultaneous measurement of both of these signals would be the only way to pin down the existence and asymmetry of the dark sector, and map out its distribution in the local cosmos.

ACKNOWLEDGMENTS

The authors would like to thank Joseph Bramante, Yue Zhao for helpful discussion. NS is supported by the

National Natural Science Foundation of China (NSFC) Project No. 12347105 and No. 12047503. QL and ACV are supported by the Arthur B. McDonald Canadian Astroparticle Physics Research Institute, with equipment funded by the Canada Foundation for Innovation and the Province of Ontario, and housed at the Queen's Centre for Advanced Computing. Research at Perimeter Institute is supported by the Government of Canada through the Department of Innovation, Science, and Economic Development, and by the Province of Ontario. ACV is also supported by NSERC, and the province of Ontario via an Early Researcher Award.

-
- [1] M. G. Aartsen *et al.* (IceCube), Evidence for High-Energy Extraterrestrial Neutrinos at the IceCube Detector, *Science* **342**, 1242856 (2013), [arXiv:1311.5238 \[astro-ph.HE\]](#).
- [2] S. L. Glashow, Resonant Scattering of Antineutrinos, *Phys. Rev.* **118**, 316 (1960).
- [3] M. G. Aartsen *et al.* (IceCube), Detection of a particle shower at the Glashow resonance with IceCube, *Nature* **591**, 220 (2021), [Erratum: Nature 592, E11 (2021)], [arXiv:2110.15051 \[hep-ex\]](#).
- [4] R. W. Brown and F. W. Stecker, Cosmic Ray Neutrino Tests for Heavier Weak Bosons and Cosmic Antimatter, *Phys. Rev. D* **26**, 373 (1982).
- [5] L. A. Anchordoqui, H. Goldberg, F. Halzen, and T. J. Weiler, Neutrinos as a diagnostic of high energy astrophysical processes, *Phys. Lett.* **B621**, 18 (2005), [arXiv:hep-ph/0410003](#).
- [6] A. Bhattacharya, R. Gandhi, W. Rodejohann, and A. Watanabe, The Glashow resonance at IceCube: signatures, event rates and pp vs. $p\gamma$ interactions, *JCAP* **10**, 017, [arXiv:1108.3163 \[astro-ph.HE\]](#).
- [7] Z.-z. Xing and S. Zhou, The Glashow resonance as a discriminator of UHE cosmic neutrinos originating from p-gamma and p-p collisions, *Phys. Rev.* **D84**, 033006 (2011), [arXiv:1105.4114](#).
- [8] V. Barger, J. Learned, and S. Pakvasa, IceCube PeV Cascade Events Initiated by Electron-Antineutrinos at Glashow Resonance, *Phys. Rev.* **D87**, 037302 (2013), [arXiv:1207.4571](#).
- [9] A. Bhattacharya, R. Gandhi, W. Rodejohann, and A. Watanabe, On the interpretation of IceCube cascade events in terms of the Glashow resonance, (2012), [arXiv:1209.2422 \[hep-ph\]](#).
- [10] L. A. Anchordoqui, T. C. Paul, L. H. M. da Silva, D. F. Torres, and B. J. Vlcek, What IceCube data tell us about neutrino emission from star-forming galaxies (so far), *Phys. Rev. D* **89**, 127304 (2014), [arXiv:1405.7648 \[astro-ph.HE\]](#).
- [11] V. Barger, L. Fu, J. G. Learned, D. Marfatia, S. Pakvasa, and T. J. Weiler, Glashow resonance as a window into cosmic neutrino sources, *Phys. Rev. D* **90**, 121301 (2014), [arXiv:1407.3255 \[astro-ph.HE\]](#).
- [12] A. Palladino, G. Pagliaroli, F. L. Villante, and F. Vissani, Double pulses and cascades above 2 PeV in IceCube, *Eur. Phys. J.* **C76**, 52 (2016), [arXiv:1510.05921](#).
- [13] L. A. Anchordoqui, M. M. Block, L. Durand, P. Ha, J. F. Soriano, and T. J. Weiler, Evidence for a break in the spectrum of astrophysical neutrinos, *Phys. Rev.* **D95**, 083009 (2017), [arXiv:1611.07905](#).
- [14] D. Biehl, A. Fedynitch, A. Palladino, T. J. Weiler, and W. Winter, Astrophysical Neutrino Production Diagnostics with the Glashow Resonance, *JCAP* **01**, 033, [arXiv:1611.07983 \[astro-ph.HE\]](#).
- [15] G.-y. Huang and Q. Liu, Hunting the Glashow Resonance with PeV Neutrino Telescopes, *JCAP* **03**, 005, [arXiv:1912.02976 \[hep-ph\]](#).
- [16] G.-y. Huang, M. Lindner, and N. Volmer, Inferring astrophysical neutrino sources from the Glashow resonance, *JHEP* **11**, 164, [arXiv:2303.13706 \[hep-ph\]](#).
- [17] Q. Liu, N. Song, and A. C. Vincent, Probing neutrino production in high-energy astrophysical neutrino sources with the Glashow resonance, *Phys. Rev. D* **108**, 043022 (2023), [arXiv:2304.06068 \[astro-ph.HE\]](#).
- [18] G.-y. Huang, Discovery potential of the Glashow resonance in an air shower neutrino telescope, (2023), [arXiv:2307.12153 \[astro-ph.HE\]](#).
- [19] F. W. Stecker, S. T. Scully, S. Liberati, and D. Mattingly, Searching for Traces of Planck-Scale Physics with High Energy Neutrinos, *Phys. Rev. D* **91**, 045009 (2015), [arXiv:1411.5889 \[hep-ph\]](#).
- [20] I. M. Shoemaker and K. Murase, Probing BSM Neutrino Physics with Flavor and Spectral Distortions: Prospects for Future High-Energy Neutrino Telescopes, *Phys. Rev.* **D93**, 085004 (2016), [arXiv:1512.07228](#).
- [21] M. Bustamante, New limits on neutrino decay from the Glashow resonance of high-energy cosmic neutrinos, (2020), [arXiv:2004.06844 \[astro-ph.HE\]](#).
- [22] D.-H. Xu and S.-J. Rong, Connect the Lorentz violation to the Glashow resonance event, *Mod. Phys. Lett. A* **38**, 2350029 (2023), [arXiv:2211.05478 \[hep-ph\]](#).
- [23] M. Blennow, E. Fernandez-Martinez, A. Olivares-Del Campo, S. Pascoli, S. Rosauero-Alcaraz, and A. V. Titov, Neutrino Portals to Dark Matter, *Eur. Phys. J. C* **79**, 555 (2019), [arXiv:1903.00006 \[hep-ph\]](#).
- [24] J. B. G. Alvey and M. Fairbairn, Linking Scalar Dark Matter and Neutrino Masses with IceCube 170922A, *JCAP* **07**, 041, [arXiv:1902.01450 \[hep-ph\]](#).
- [25] S. Baumholzer, V. Brdar, P. Schwaller, and A. Segner,

- Shining Light on the Scotogenic Model: Interplay of Colliders and Cosmology, *JHEP* **09**, 136, [arXiv:1912.08215 \[hep-ph\]](#).
- [26] C. Boehm, Y. Farzan, T. Hambye, S. Palomares-Ruiz, and S. Pascoli, Is it possible to explain neutrino masses with scalar dark matter?, *Phys. Rev. D* **77**, 043516 (2008), [arXiv:hep-ph/0612228](#).
- [27] M. Escudero, N. Rius, and V. Sanz, Sterile neutrino portal to Dark Matter I: The $U(1)_{B-L}$ case, *JHEP* **02**, 045, [arXiv:1606.01258 \[hep-ph\]](#).
- [28] Y. Farzan and E. Ma, Dirac neutrino mass generation from dark matter, *Phys. Rev. D* **86**, 033007 (2012), [arXiv:1204.4890 \[hep-ph\]](#).
- [29] Y. Farzan and S. Palomares-Ruiz, Dips in the Diffuse Supernova Neutrino Background, *JCAP* **06**, 014, [arXiv:1401.7019 \[hep-ph\]](#).
- [30] H. H. Patel, S. Profumo, and B. Shakya, Loop dominated signals from neutrino portal dark matter, *Phys. Rev. D* **101**, 095001 (2020), [arXiv:1912.05581 \[hep-ph\]](#).
- [31] C. Garcia-Cely and J. Heeck, Neutrino Lines from Majoron Dark Matter, *JHEP* **05**, 102, [arXiv:1701.07209 \[hep-ph\]](#).
- [32] R. Coy and T. Hambye, Neutrino lines from DM decay induced by high-scale seesaw interactions, *JHEP* **05**, 101, [arXiv:2012.05276 \[hep-ph\]](#).
- [33] C. A. Argüelles, A. Kheirandish, and A. C. Vincent, Imaging Galactic Dark Matter with High-Energy Cosmic Neutrinos, *Phys. Rev. Lett.* **119**, 201801 (2017), [arXiv:1703.00451 \[hep-ph\]](#).
- [34] C. A. Argüelles, A. Diaz, A. Kheirandish, A. Olivares-Del-Campo, I. Safa, and A. C. Vincent, Dark matter annihilation to neutrinos, *Rev. Mod. Phys.* **93**, 035007 (2021), [arXiv:1912.09486 \[hep-ph\]](#).
- [35] C. A. Argüelles, D. Delgado, A. Friedlander, A. Kheirandish, I. Safa, A. C. Vincent, and H. White, Dark matter decay to neutrinos, *Phys. Rev. D* **108**, 123021 (2023), [arXiv:2210.01303 \[hep-ph\]](#).
- [36] D. E. Kaplan, M. A. Luty, and K. M. Zurek, Asymmetric Dark Matter, *Phys. Rev. D* **79**, 115016 (2009), [arXiv:0901.4117 \[hep-ph\]](#).
- [37] E. Nardi, F. Sannino, and A. Strumia, Decaying Dark Matter can explain the e^+ excesses, *JCAP* **01**, 043, [arXiv:0811.4153 \[hep-ph\]](#).
- [38] S. Chang and L. Goodenough, Charge Asymmetric Cosmic Ray Signals From Dark Matter Decay, *Phys. Rev. D* **84**, 023524 (2011), [arXiv:1105.3976 \[hep-ph\]](#).
- [39] I. Masina and F. Sannino, Charge Asymmetric Cosmic Rays as a probe of Flavor Violating Asymmetric Dark Matter, *JCAP* **09**, 021, [arXiv:1106.3353 \[hep-ph\]](#).
- [40] I. Masina, P. Panci, and F. Sannino, Gamma Ray Constraints on Flavor Violating Asymmetric Dark Matter, *JCAP* **12**, 002, [arXiv:1205.5918 \[astro-ph.CO\]](#).
- [41] I. Masina and F. Sannino, Hints of a Charge Asymmetry in the Electron and Positron Cosmic-Ray Excesses, *Phys. Rev. D* **87**, 123003 (2013), [arXiv:1304.2800 \[hep-ph\]](#).
- [42] L. Feng and Z. Kang, Decaying Asymmetric Dark Matter Relaxes the AMS-Fermi Tension, *JCAP* **10**, 008, [arXiv:1304.7492 \[hep-ph\]](#).
- [43] Y. Zhao and K. M. Zurek, Indirect Detection Signatures for the Origin of Asymmetric Dark Matter, *JHEP* **07**, 017, [arXiv:1401.7664 \[hep-ph\]](#).
- [44] B. Feldstein and A. L. Fitzpatrick, Discovering Asymmetric Dark Matter with Anti-Neutrinos, *JCAP* **09**, 005, [arXiv:1003.5662 \[hep-ph\]](#).
- [45] H. Fukuda, S. Matsumoto, and S. Mukhopadhyay, Asymmetric dark matter in early Universe chemical equilibrium always leads to an antineutrino signal, *Phys. Rev. D* **92**, 013008 (2015), [arXiv:1411.4014 \[hep-ph\]](#).
- [46] R. Abbasi *et al.* (IceCube), The IceCube high-energy starting event sample: Description and flux characterization with 7.5 years of data, *Phys. Rev. D* **104**, 022002 (2021), [arXiv:2011.03545 \[astro-ph.HE\]](#).
- [47] R. Abbasi *et al.* (IceCube), Improved Characterization of the Astrophysical Muon–neutrino Flux with 9.5 Years of IceCube Data, *Astrophys. J.* **928**, 50 (2022), [arXiv:2111.10299 \[astro-ph.HE\]](#).
- [48] S. D. Thomas, Baryons and dark matter from the late decay of a supersymmetric condensate, *Phys. Lett. B* **356**, 256 (1995), [arXiv:hep-ph/9506274](#).
- [49] R. Kitano and I. Low, Dark matter from baryon asymmetry, *Phys. Rev. D* **71**, 023510 (2005), [arXiv:hep-ph/0411133](#).
- [50] J. Unwin, Exodus: Hidden origin of dark matter and baryons, *JHEP* **06**, 090, [arXiv:1212.1425 \[hep-ph\]](#).
- [51] P. Asadi, E. D. Kramer, E. Kuflik, G. W. Ridgway, T. R. Slatyer, and J. Smirnov, Accidentally Asymmetric Dark Matter, *Phys. Rev. Lett.* **127**, 211101 (2021), [arXiv:2103.09822 \[hep-ph\]](#).
- [52] N. Hiroshima, R. Kitano, K. Kohri, and K. Murase, High-energy neutrinos from multibody decaying dark matter, *Phys. Rev. D* **97**, 023006 (2018), [arXiv:1705.04419 \[hep-ph\]](#).
- [53] P. F. de Salas, K. Malhan, K. Freese, K. Hattori, and M. Valluri, On the estimation of the Local Dark Matter Density using the rotation curve of the Milky Way, *JCAP* **10**, 037, [arXiv:1906.06133 \[astro-ph.GA\]](#).
- [54] I. Esteban, M. C. Gonzalez-Garcia, M. Maltoni, T. Schwetz, and A. Zhou, The fate of hints: updated global analysis of three-flavor neutrino oscillations, *JHEP* **09**, 178, [arXiv:2007.14792 \[hep-ph\]](#).
- [55] NuFIT 5.3 (2024), <http://www.nu-fit.org/?q=node/278> (2021).
- [56] N. Aghanim *et al.* (Planck), Planck 2018 results. VI. Cosmological parameters, *Astron. Astrophys.* **641**, A6 (2020), [Erratum: *Astron. Astrophys.* 652, C4 (2021)], [arXiv:1807.06209 \[astro-ph.CO\]](#).
- [57] C. W. Bauer, N. L. Rodd, and B. R. Webber, Dark matter spectra from the electroweak to the Planck scale, *JHEP* **06**, 121, [arXiv:2007.15001 \[hep-ph\]](#).
- [58] T. Sjöstrand, S. Mrenna, and P. Z. Skands, PYTHIA 6.4 Physics and Manual, *JHEP* **05**, 026, [arXiv:hep-ph/0603175](#).
- [59] T. Sjöstrand, S. Mrenna, and P. Z. Skands, A Brief Introduction to PYTHIA 8.1, *Comput. Phys. Commun.* **178**, 852 (2008), [arXiv:0710.3820 \[hep-ph\]](#).
- [60] T. Sjöstrand, S. Ask, J. R. Christiansen, R. Corke, N. Desai, P. Ilten, S. Mrenna, S. Prestel, C. O. Rasmussen, and P. Z. Skands, An introduction to PYTHIA 8.2, *Comput. Phys. Commun.* **191**, 159 (2015), [arXiv:1410.3012 \[hep-ph\]](#).
- [61] A. Loewy, S. Nussinov, and S. L. Glashow, The Effect of Doppler Broadening on the 6.3 PeV W^- Resonance in $\bar{\nu}_e e^-$ Collisions, (2014), [arXiv:1407.4415 \[hep-ph\]](#).
- [62] W. D. Apel *et al.* (KASCADE Grande), KASCADE-Grande Limits on the Isotropic Diffuse Gamma-Ray Flux between 100 TeV and 1 EeV, *Astrophys. J.* **848**, 1 (2017), [arXiv:1710.02889 \[astro-ph.HE\]](#).
- [63] M. G. Aartsen *et al.* (IceCube), Differential limit on

- the extremely-high-energy cosmic neutrino flux in the presence of astrophysical background from nine years of IceCube data, *Phys. Rev. D* **98**, 062003 (2018), [arXiv:1807.01820 \[astro-ph.HE\]](#).
- [64] Z. Cao *et al.* (LHAASO), Constraints on Heavy Decaying Dark Matter from 570 Days of LHAASO Observations, *Phys. Rev. Lett.* **129**, 261103 (2022), [arXiv:2210.15989 \[astro-ph.HE\]](#).
- [65] M. G. Aartsen *et al.* (IceCube-Gen2), IceCube-Gen2: the window to the extreme Universe, *J. Phys. G* **48**, 060501 (2021), [arXiv:2008.04323 \[astro-ph.HE\]](#).
- [66] S. Adrian-Martinez *et al.* (KM3Net), Letter of intent for KM3NeT 2.0, *J. Phys. G* **43**, 084001 (2016), [arXiv:1601.07459 \[astro-ph.IM\]](#).
- [67] A. D. Avrorin *et al.* (Baikal-GVD), Baikal-GVD: status and prospects, *EPJ Web Conf.* **191**, 01006 (2018), [arXiv:1808.10353 \[astro-ph.IM\]](#).
- [68] M. Agostini *et al.* (P-ONE), The Pacific Ocean Neutrino Experiment, *Nature Astron.* **4**, 913 (2020), [arXiv:2005.09493 \[astro-ph.HE\]](#).
- [69] J. P. Twagirayezu, H. Niederhausen, S. Sclafani, N. Whitehorn, M. Nisa, S. Yu, and R. Halliday (P-ONE), Performance of the Pacific Ocean Neutrino Experiment (P-ONE), *PoS ICRC2023*, 1175 (2023).
- [70] Z. P. Ye *et al.*, Proposal for a neutrino telescope in South China Sea, (2022), [arXiv:2207.04519 \[astro-ph.HE\]](#).
- [71] T.-Q. Huang, Z. Cao, M. Chen, J. Liu, Z. Wang, X. You, and Y. Qi, Proposal for the High Energy Neutrino Telescope, *PoS ICRC2023*, 1080 (2023).
- [72] R. Gauld, Precise predictions for multi-TeV and PeV energy neutrino scattering rates, *Phys. Rev. D* **100**, 091301 (2019), [arXiv:1905.03792 \[hep-ph\]](#).
- [73] A. Garcia, R. Gauld, A. Heijboer, and J. Rojo, Complete predictions for high-energy neutrino propagation in matter, *JCAP* **09**, 025, [arXiv:2004.04756 \[hep-ph\]](#).

Appendix A: Neutrino distribution function in dark matter decay

Here we discuss the initial spectra of the neutrino production via our benchmark decay modes. In a two-body decay, the monoenergetic initial states from the decay can be described by a delta function $df_i/dy = \delta(y - y_{i,0})$. Here y represents the energy fraction taken away by particle i . For benchmarks B1 and B2, when $m_\psi \ll m_X$, $y_{i,0} = 1/2$ for all decay products. If $m_\psi \lesssim m_X$ instead, $y_{\nu,0} = (m_X^2 - m_\psi^2)/(2m_X^2)$. Therefore, the B1 neutrino spectrum matches the spectrum of B2 at mass $m'_X = 2y_0 m_X$ with the normalization reduced by a factor of 2.

For a multi-body decay mode $X \rightarrow \nu + 2n\psi$, in the massless limit $m_\psi \ll m_X$, the distribution function of ν is [52]

$$\frac{df_\nu}{dy} = 4N(N-1)(N-2)y^2(1-2y)^{N-3}, \quad (\text{A1})$$

where $N \equiv 3n + 1$ and $y \in [0, \frac{1}{2}]$. The distribution function of each product ψ in the pairs is

$$\frac{df_\psi}{dy} = 8N(N-1)(N-2)(1-2y)^2(4y-1)^{N-3}, \quad (\text{A2})$$

where $y \in [\frac{1}{4}, \frac{1}{2}]$. In benchmark B3, ψ is a dark particle, and it does not contribute to the neutrino flux. In benchmark B4, $\psi = \nu$ instead, and the $\nu(\bar{\nu})$ distribution is obtained by adding up Eq. (A1) and Eq. (A2). As no matter whether L_X is negative or positive, the neutrino pair contributes the same to the spectrum, making the final spectra close to each which weakens the power of GR. It is also possible that the n ψ pairs are other SM particle pairs, and they can eventually produce neutrinos through hadronization, decay or radiative processes. The exploration of this scenario is left for future work.

Appendix B: Sensitivity of dark matter decay with next generation of neutrino telescopes

Fig. 3 shows the evolution of the sensitivity for $m_X = 20$ PeV as the exposure grows for the representative decay channels. The projected sensitivity approximately follows $\tau_X/\tau_0 \simeq \mathcal{E}^{0.59}$, where \mathcal{E} is the exposure of the experiment and τ_0 depends on the channel. For B2 $X \rightarrow \bar{\nu}\bar{\nu}(\nu\nu)$, $\tau_0 \simeq 10^{28.3}(10^{27.7})$ s. For B3 $X \rightarrow \bar{\nu}(\nu)+\psi\psi$, $\tau_0 \simeq 10^{28.3}(10^{26.9})$ s. For B4 $X \rightarrow \bar{\nu}(\nu) + \nu\bar{\nu}$, $\tau_0 \simeq 10^{28.8}(10^{28.6})$ s.

At the top, the approximate 10 yr exposure timelines of next-generation telescopes are marked. These are mainly based on sensitivities presented before full experimental details or funding were finalized. We keep these numbers here, as up-to-date sensitivities have not been published. In addition to IceCube-Gen2, the high-energy module of KM3NeT [66] will be instrumented with two 115-string arrays, which in combination provides an effective volume of 2.8 km³. Although Baikal-GVD has been taking data since 2018 [67], the detector is expected finally reach an instrumented volume of 1.5 km³. P-ONE [68], a planned water-Cherenkov detector in the north-eastern Pacific Ocean, will be constructed with an estimated volume of 3.2 km³, although more recent conference presentations suggest a smaller volume [69]. TRIDENT [70], proposed to be built in the South China Sea, is partially funded and has an ultimate goal of reaching 7.5 km³. For the combined exposure of neutrino telescopes by 2040, it is based on the approximate timeline that the full configuration of Baikal-GVD and KM3NeT will start taking data in 2025 while IceCube-Gen2, P-ONE and TRIDENT will be turned on in 2030, corresponding to an exposure of 19 yr for IceCube, 15 yr for Baikal-GVD and KM3NeT, and 10 yr for P-ONE, TRIDENT and IceCube-Gen2 respectively. The volumes and timelines we have adopted for upcoming detectors are tentative and subject to changes, and may be augmented by the instrumentation of even larger detectors, such as the recently proposed HUNT [71]. As the normalization of the lifetime sensitivity scales with the exposure while the shapes approximately keeps the same with varying mass, the projected sensitivity lines in Fig. 2 can be scaled to obtain the sensitivity lines with any more realistic exposure in the future.

Appendix C: Effects of corrections on the GR cross section

Following the increasing number of studies on high-energy neutrino interactions, subleading effects are being considered when computing cross sections. For GR cross sections, the discussed corrections are from the Doppler broadening [61] and the initial photon radiation [72, 73]. These effects lead to a $\sim 30\%$ drop at the resonant energy, a slight broadening and higher values above the resonant energy of the cross section [16]. The former has been implemented in the IceCube GR analysis [3]. As the effective area of contained or partially contained events is approximately proportional to the cross section, the effect on the event rate can be estimated. Here, with the HESE MC, we can

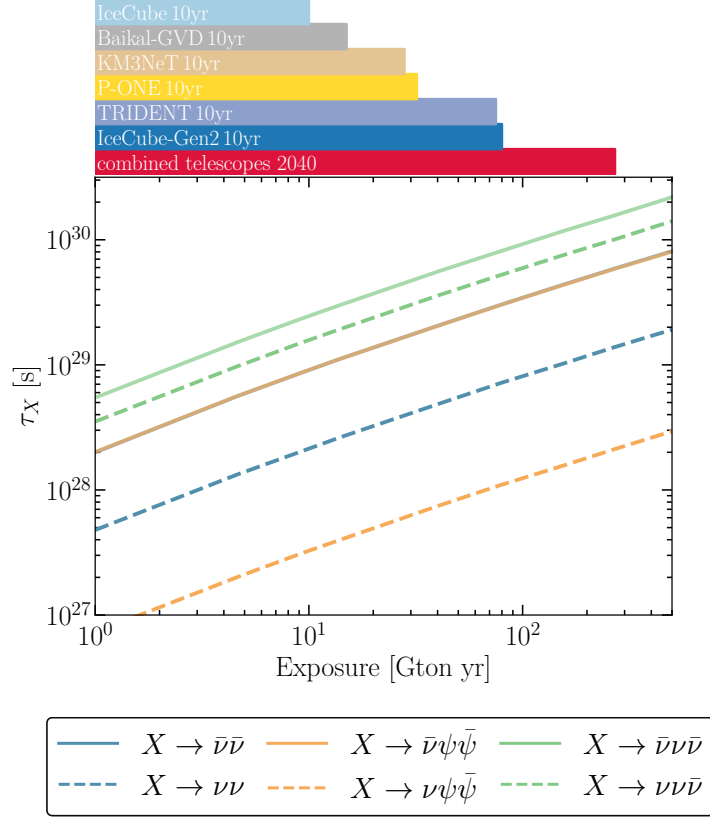


FIG. 3. The sensitivity evolution with the exposure for the three different decay modes for $m_X = 20$ PeV. Solid lines correspond to negative lepton numbers and dashed lines correspond to positive lepton numbers (the $X \rightarrow \bar{\nu}\nu$ line accidentally coincides with $X \rightarrow \bar{\nu}\psi\bar{\psi}$ at $m_X = 20$ PeV). The bars on the top indicate the 10 yr exposure of IceCube and next-generation neutrino telescopes. The red bar corresponds to an estimated exposure in year 2040 with combined neutrino telescopes which are composed of 19 yr IceCube, 15 yr Baikal-GVD+KM3NeT and 10 yr P-ONE+TRIDENT+IceCube-Gen2.

obtain the effective area incorporating the two effects by scaling the MC weight of each simulated event by the ratio of the modified cross section and the original cross section. With the 3 energy bins discussed above, the first 2 bins have a negligible change with a drop by less than several percent while for the bin above the resonant energy there is a 20%-30% increase for a power-law spectrum.

We check the effect of the cross section corrections on the constraints on ADM, and find an improvement at only a level of several percent in the DM lifetime, which is negligible. The improvement is less significant compared to the change in the event rate, since the GR event rates from DM decay and diffuse astrophysical neutrino flux both change similarly due to the cross section corrections.